

Autonomous piston engine guided by the transduction of radiation pressure in optomechanical Brownian motors

Yusuf GÜL^{1,2,*} 

¹Institute of Biomedical Engineering, Boğaziçi University, İstanbul, Turkey

²Department of Physics, Boğaziçi University, İstanbul, Turkey

Received: 09.06.2018

Accepted/Published Online: 15.01.2019

Final Version: 22.02.2019

Abstract: We consider the autonomous piston engine in a coupled cavity scheme in an optomechanical setup. Treating the radiation field as working fluid, we investigate the transduction of virtual photons due to ground state excitations. Rabi-like energy splittings and Casimir effect are shown by avoided crossing in the eigenfunction spectrum. Second order coherence functions are employed to analyze the bunching of the cavity and mechanical mode in optomechanical implementation of Brownian motors. The imbalance in occupation numbers of the working modes is investigated for the power for work extraction. We explore the guidance of the radiation field in work extraction. We study the synchronicity between virtual photon conversion and power in the mechanical mode. Generation and amplification of virtual photon transduction are modulated by mutual interactions between the qubit, piston, and mechanical mode in the absence of external driving fields.

Key words: Stochastic thermodynamics, optomechanics, cavity QED

1. Introduction

Stochastic thermodynamics allows the description of the conversion of thermal fluctuations into mechanical work on small scales, such as in Brownian Carnot engines [1–5] and artificial motors [6]. Moreover, miniaturized heat engines are implemented in microscale realization of photon–matter interactions [7–11]. In different coupling regimes of optomechanical systems, transfers of the cavity photons are used to describe energy conversion by the radiation pressure interactions [12].

Autonomous design of thermal machines gives rise to exploration of the fundamental principles of quantum thermodynamics. Realizations of autonomous engines can be implemented in the absence of external control fields [13–16]. In quantum autonomous architectures [17, 18], the piston is represented as a planar rotor coupled with the harmonic mode treated as working fluid. In analogy with the classical counterparts [19, 20], these engines are guided by the radiation pressure by modulating the coupling strengths of hot and cold reservoirs in the rotor engine scheme. Depending on the energy transfer in bipartite systems, states can be treated as both heat and work resources [21, 22]. Lasing process [23] and Jarzynski equality [24] are used in the Jaynes–Cummings model as a bipartite system of qubit and radiation field. Work extraction can be described by the average excitation numbers of individual cavity modes coupled to hot and cold baths. Besides the thermal reservoirs, additional resources can be used for work extraction from quantum states by membrane optomechanical systems [25] and Cooper pair tunneling in Josephson junctions [26].

*Correspondence: yusufgul.josephrose@gmail.com

In the enhancement of optomechanical-like interactions, external fields are used for mechanical amplifications by modulating nonlinear interactions [27]. Dynamical Casimir effect and virtual photon radiation are investigated to describe the displacement of the mechanical mode [28]. Jaynes–Cummings-like and Rabi-like interactions are employed in single mode [29, 30] and fully coupled optomechanical systems [31]. Moreover, in strong coupling regimes, the ground state becomes dressed with virtual photons [32–34]. Then the system is described by going beyond to rotating wave approximation (RWA) [35–38]. Effective models [39–41] are used to describe the coupled resonator systems without RWA in input–output formalism [42, 43]. Global and local approaches are also employed to investigate the thermodynamic analysis of the systems [44–47].

This paper is organized as follows. In Section 2, we introduce the enhancement of autonomous optomechanical-like interactions in fully coupled schemes by an effective coupled resonator model. Results and conclusions are introduced in Sections 3 and 4, respectively.

2. Model

Fully coupled optomechanical systems contain the mutual interactions between qubit, cavity, and mechanical mode. Coupling between the cavity photons and the qubit describes the cavity frequency shift due to a displacement of the mechanical resonator. Radiation–pressure coupling is used to modulate the interaction between the cavity mode and mechanical motion. Similar to the scheme in [31], our model Hamiltonian is ($\hbar = 1$)

$$H_{sys} = H_{OM} + H_{CR}, \quad (2.1)$$

where

$$H_{OM} = \omega_1 a_1^\dagger a_1 + \omega_2 a_2^\dagger a_2 - J a_1^\dagger a_1 (a_2 + a_2^\dagger) \quad (2.2)$$

is the optomechanical Hamiltonian and

$$H_{CR} = \frac{\omega}{2} \sigma_z + [\lambda_1 (a_1 + a_1^\dagger) + \lambda_2 (a_2 + a_2^\dagger)] \sigma_x \quad (2.3)$$

is the Hamiltonian containing counter-rotating terms, which describes the Rabi-type interactions with the qubit. ω is the frequency of the qubit and σ_x, σ_z are the Pauli operators. The cavity and mechanical system are described by the annihilation (creation) operators $a_i (a_i^\dagger)$, where $i = 1, 2$ corresponds to the cavity and mechanical mode. $\omega_{1,2}$ are the frequencies of the radiation field of the cavity and mechanical mode. The qubit is simultaneously coupled to cavity and mechanical modes with coupling strengths $\lambda_{1,2}$. Interaction between the cavity field and mechanical oscillator is modulated by the parameter J . Rather than being fully coupled in tripartite systems, binary interactions of the qubit and optomechanical mode are used in tunable photon blockades of two-mode optomechanical systems [29]. Besides the Rabi-like interactions, binary cavity–mechanical mode interactions are tuned for amplification of virtual radiation pressure [30].

In accordance with the classical counterpart, we describe the piston–mechanical mode interaction by the coupling between radiation pressure and mechanical mode. Bouncing of the photons off the mechanical part resembles the behavior of the photon gas contained in the cavity. Besides this classical analogy, in the presence of the virtual photons, we use radiation pressure to amplify the mechanical motion. In autonomous engine design [17–20], both qubit and harmonic mode are treated as working fluid and amplified by the nonlinear

interactions autonomously. Then our model is well suited to investigate the embodiment of a fully coupled optomechanical scheme in autonomous engine design. For this purpose, we employ the two-frequency effective coupled resonator model [39–41] and describe our system as

$$H = H_{eff} + H_{int}, \quad (2.4)$$

where the effective Hamiltonian becomes

$$\begin{aligned} H_{eff} = & \frac{\omega}{2}\sigma_z + \omega'\alpha_2^\dagger\alpha_2 + \omega_{eff}[\alpha_1^\dagger\alpha_1 + k_{eff}(\alpha_1 + \alpha_1^\dagger)\sigma_x] \\ & + c_2[(\alpha_1^\dagger\alpha_2 + \alpha_1\alpha_2^\dagger) + k_{eff}(\alpha_2^\dagger + \alpha_2)\sigma_x], \end{aligned} \quad (2.5)$$

and the radiation–pressure interaction is obtained as

$$\begin{aligned} H_{int} = & J[(\alpha_1^\dagger\alpha_2 + \alpha_2^\dagger\alpha_1) + (\alpha_1 + \alpha_2)^\dagger(\alpha_2^2 - \alpha_1^2) \\ & + (\alpha_1 + \alpha_2)(\alpha_2^2 - \alpha_1^2)^\dagger]. \end{aligned} \quad (2.6)$$

The effective mode frequency is described as

$$\omega_{eff} = \frac{\omega_1 k_1^2 + \omega_2 k_2^2}{k_{eff}^2}. \quad (2.7)$$

The qubit–resonator coupling strength becomes proportional to

$$k_{eff}^2 = k_1^2 + k_2^2 \quad (2.8)$$

in terms of the dimensionless coupling coefficients $k_{1,2}$. The frequency of the disadvantaged mode in the effective model is obtained as

$$\omega' = \frac{\omega_1 k_2^2 + \omega_2 k_1^2}{k_{eff}^2}, \quad (2.9)$$

and the coupling strength,

$$c_2 = \frac{\Delta k_1 k_2}{k_{eff}^2}, \quad (2.10)$$

describes interactions between the disadvantaged and the privileged mode controlled by the the frequency difference $\Delta = \omega_1 - \omega_2$. For simulation in the effective model [41–43], we use the parameters of $k_1 = k_1 = k$, resulting in $k_{eff} = \sqrt{2}k$. In terms of the bare resonances $\omega_{1,2}$, the coupling strengths are taken as $\lambda_1 = (\omega_1 + \omega_1)k/2$ and $\lambda_2 = \Delta k/2$. The hopping parameter is written as $J = c_2 = \Delta/2$.

Our effective model is plausible for investigating the mechanical properties of the coupled system via both cavity and circuit QED framework. One of the advantages of our model is that we can still obtain the single mode qubit–cavity interactions by tuning $\lambda_2 = \Delta k/2 = 0$ and $c_2 = 0$, corresponding to $\omega_1 = \omega_2$. Then our model mimics the optomechanical-like single mode qubit–cavity or qubit–mechanical mode interactions [29, 30].

Besides this flexibility, Casimir force and Rabi splitting can be investigated by the Rabi-like interactions in the fully coupled scheme of our effective model. Interaction between radiation pressure and mechanical mode, described by hopping parameter J , gives rise to the modulation of the virtual photon transduction by the displacement of the mechanical probe. In view of autonomous engine architectures, our effective model treats the cavity and mechanical mode as high and low frequency mode, respectively. Then energy transfer is described by the occupation number of cavity and mechanical modes in the quantum piston engines. Imbalances in occupation numbers of the working modes result in the power for work extraction.

3. Results

In optomechanical systems, radiation pressure force allows the energy exchange between cavity and mechanical displacements. Then the generation of photons from the quantum vacuum is amplified with controllable coupling strengths of radiation pressure [30]. We investigated the Rabi-like energy splittings and Casimir effect [28] in the eigenvalue spectrum to see the virtual photon generation controlled by frequency differences between cavity and mechanical mode. By using $J = c_2 = \Delta/2$, we can modulate the pattern of the avoided crossings in the absence of external driving fields. Then our model can be treated as an autonomous system in which both Rabi-like and nonlinear interactions can be used for field amplification.

The eigenvalue spectrum of our system is analyzed in the five lowest levels for weak and strong coupling regimes. In Figure 1, we investigate the effect of hopping parameter J . The ladder of avoiding crossings represents how the Casimir effect and Rabi splitting depend on frequency difference Δ . Figure 1a shows the avoided crossing for each level with increasing number of anticrossings as a function of frequency difference Δ in weak coupling regime, $k = 0.1$ and $J = 0.1$. The effect of radiation–pressure interaction is seen by the shift of the pattern in Figure 1b. As we increase the coupling strengths of the cavity field and mechanical mode, from $k = 0.1$ and $J = 0.1$ to $k = 0.1$ and $J = 1.0$, the number of anticrossings is also increasing and avoided crossing occurs in smaller Δ values. In Figure 1c, the level splitting increases as an indication of Casimir effect when we go to the strong coupling regime, $k = 1.0$ and $J = 1.0$.

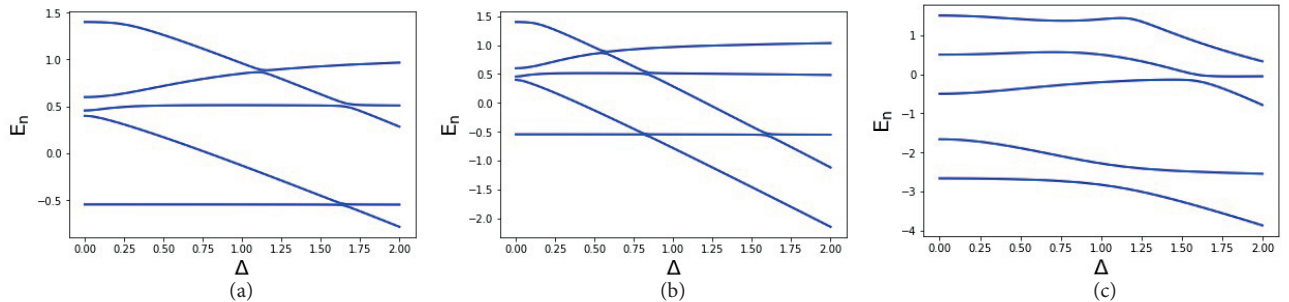


Figure 1. Ladder of avoiding level crossings in the eigenvalue spectrum of our system. Visible anticrossings imply the generation of photons from the vacuum. (a) Avoiding crossing in the presence of nonlinear interaction with $k = 0.1$ and $J = 0.1$. (b) Effect of increasing the coupling strength in the number of anticrossings with $k = 0.1$ and $J = 1.0$. (c) Level splitting due to the dynamical Casimir effect in strong coupling regime $k = 1.0$ and $J = 1.0$.

In input–output formalism of dissipative cavity optomechanics, quantum piston engines are studied in classical and quantum regimes when the working fluids are in harmonic mode [19] and qubit [20]. In our model, treating the harmonic mode as working fluid, piston–qubit interaction terms $\omega_{eff}k_{eff}(\alpha_1 + \alpha_1^\dagger)\sigma_x$ and $c_2k_{eff}(\alpha_2 + \alpha_2^\dagger)\sigma_x$ result in the virtual photon generation. Moreover, piston–mechanical mode interaction

$J(\alpha_1^\dagger\alpha_2 + \alpha_2^\dagger\alpha_1)$ makes it possible to transfer the radiation field between cavity and mechanical mode. In this way, both virtual photon generation [32–34] and energy transfer by radiation pressure [19, 20] become integrated in our model.

Thus, the dissipative environmental effects are analyzed by the master equation in the QED framework. The local approach [44–47] is used in our scheme since we use thermal white noise resulting in low thermal occupancy with respect to frequencies of the cavity and optomechanical modes. We use the Bloch–Redfield quantum master equation in Born–Markov approximation [41–43] for Eq. (2.4). Then the governing equation for the open dissipative system is written as

$$\frac{d\rho}{dt} = -i[H, \rho] + \mathcal{L}\rho, \quad (3.1)$$

where the Liouvillian superoperator \mathcal{L} is described by

$$\begin{aligned} \mathcal{L}\rho &= \sum_{j=1,2} (1 + n_{th})\kappa\mathcal{D}[\hat{a}_j]\rho + n_{th}\kappa\mathcal{D}[\hat{a}_j^\dagger]\rho \\ &+ \gamma\mathcal{D}[\sigma]\rho + \frac{\gamma_\phi}{2}\mathcal{D}[\sigma_z]\rho, \end{aligned} \quad (3.2)$$

where n_{th} represents the average thermal photon number. In our simulations of dissipation effects, taking the value $n_{th} = 0.15$ corresponds to 100 mK [41]. \mathcal{D} represents the Lindblad-type damping superoperators and κ denotes loss rate. Relaxation and dephasing rates of the qubit are γ and γ_ϕ . We take resonator decay parameters $\kappa_1 = \kappa_2 = 0.001$ and qubit relaxation and dephasing parameters $\gamma = 0.001, \gamma_\phi = 0.01$ with the thermal occupation number $n_{th} = 0.15$. For robustness in computation, each resonator mode has Fock space dimension 2.

Following the idea of production of thermodynamic work of a ratchet machine by extracting from random Brownian noise [6], our effective model is treated as a Brownian motor [17]. In piston engines, to investigate the lasing regime of mechanical mode and absorption of the photons, we employ the second order coherence functions given by

$$g_i^{(2)} = \frac{O_i^\dagger(t)O_i^\dagger(t+\tau)O_i(t)O_i(t+\tau)}{(O_i^\dagger(t)O_i(t))^2}, \quad (3.3)$$

where $i = c, d$ are used in place of cavity, α_1 , and mechanical probe mode, α_2 .

For the purposes of the conversion between radiation and mechanical mode, we use the displacement operators $X_i^+ = \frac{1}{2}(a_i + a_i^\dagger)$, where $i = 1, 2$ represents the resonators in the coupled scheme of the optomechanical system. Then, in terms of the normal modes $\alpha_{1,2}$ of our effective model [42, 43], we use the quadrature operators $X_1^+ = (\alpha_1 + \alpha_1^\dagger)$ and $X_2^+ = (\alpha_2 + \alpha_2^\dagger)$ to investigate the transduction of the radiation pressure into the mechanical motion in the presence of virtual photons and multilevel excitations [28, 30].

In autonomous engines, work extraction is studied by the power P related to output work in terms of the expectation values of number operators [17, 26]. For this purpose, we use the population imbalances $z_q(\tau) = \langle X_1^+ \rangle - \langle X_2^+ \rangle$ and $z_n(\tau) = \langle \alpha_1 \rangle - \langle \alpha_2 \rangle$ in terms of the expectation values of quadrature operators $X_{1,2}^+$ and normal modes $\alpha_{1,2}$. Then the power related to the work output will be proportional to the population imbalances $P \propto z_n$. We can also describe energy transfer as the energy change proportional to a change in

mode occupation of radiation mode, which is treated as working fluid. We use the population imbalance of the cavity quadrature operator z_q to analyze the generation of virtual photons and conversion to the mechanical motion. Then coupling strength k and hopping parameter J are used to analyze the work extraction in the presence of virtual photon generation and conversion.

In Figure 2, starting with a single photon residing in resonator mode α_1 , we investigate the population imbalances and second order coherence functions $g_{c,d}^{(2)}$ of the cavity and mechanical mode in weak $k = 0.5$ and strong $k = 1.0$ coupling regimes. In Figures 2a–2d, $g_d^{(2)}(g_c^{(2)})$ starts from the bunching (antibunching) states of mechanical mode (cavity mode). In the long term, convergence to coherence $g_{c,d}^{(2)} = 1$ indicates the coherent mechanical motion and cavity field. Since a single photon resides in radiation mode α_1 initially, incoherent effects are seen in the beginning of the evolution. In this short duration, both population imbalances reach their maximum amplitude. Then both z_q and z_n show peaks and dips as both coherence functions reach bunching, $g_{c,d}^{(2)} = 1$. Figure 2a shows that there is less contribution to the virtual photon generation for a slightly short time. Population imbalance of normal modes, $z_n(\tau) = \langle \alpha_1 \rangle - \langle \alpha_2 \rangle$, gets centered a slight bit above (below) zero in the weak coupling regime, $k = 0.5$, $J = 1.0$. When we change the hopping parameter from $k = 0.5$, $J = 1.0$ to $k = 0.5$, $J = 1.0$ in Figure 2b, the amplitude of z_q gets larger, favoring the mechanical mode in the

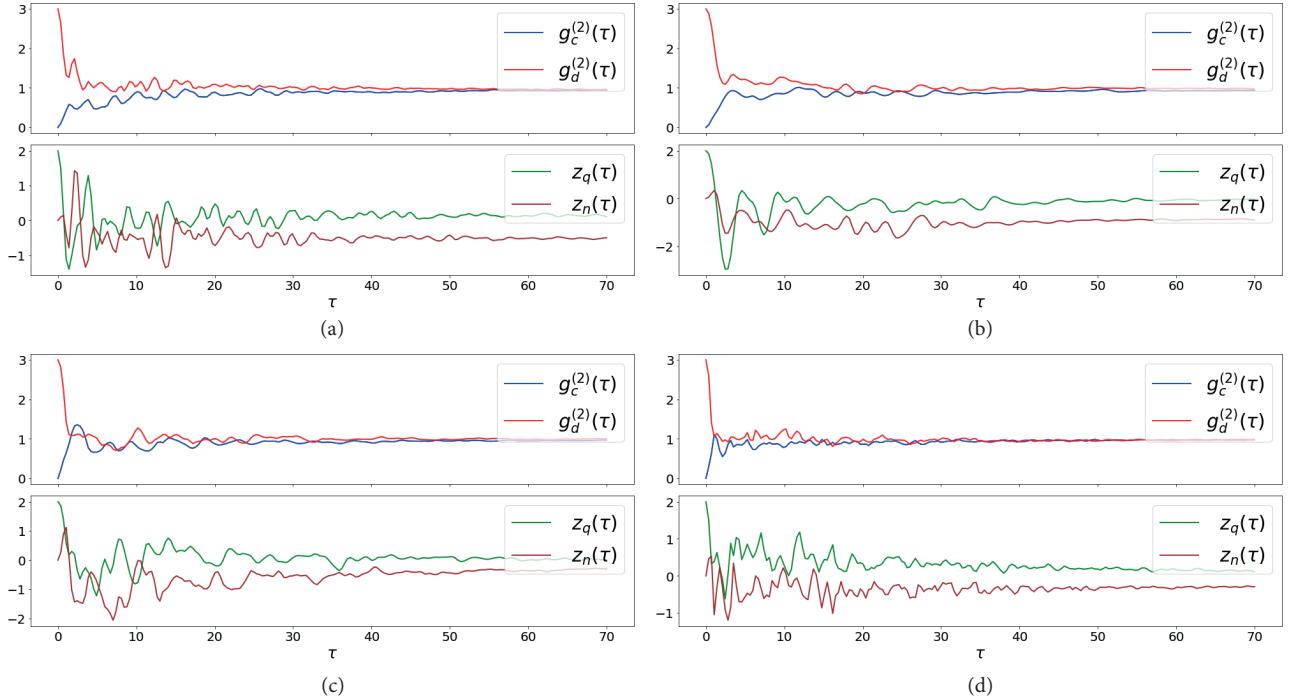


Figure 2. Conversion of photon energy into the coherent mechanical motion. Synchronicity in population differences of quadrature operators and normal modes implies the guidance of the work extraction by radiation pressure. Convergence of coherence functions $g_{c,d}^{(2)} = 1$ shows the lasing of the mechanical mode and coherence of the cavity field in weak and strong coupling regimes. (a) Expectation values of population imbalances in weak coupling regime. Conversion of virtual photons in favor of mechanical mode. (b) Effect of decreasing nonlinear coupling strength parameter J on population imbalances. There is no net favor of virtual photon conversion on population imbalances. (c) Synchronicity is seen by the coincidence of the peak and dip values of population imbalances. Virtual photon conversion is in favor of mechanical mode with higher amplitude in strong coupling regime. (d) Decreasing hopping parameter J results in less coincidence of the peak and dip values of population imbalances.

beginning of the evolution. In the strong coupling regime, $k = 0.5$ and $J = 1.0$, as both coherence functions $g_{c,d}^{(2)}$ are in the bunching regime, Figure 2c shows that synchronicity occurs in peak and dip values of population imbalances z_q and z_n . Moreover, there is virtual photon generation and conversion into the mechanical mode with higher amplitudes than in the weak regime. In Figure 2d, while there is more contribution to the virtual photon contribution, the amplitude of the population imbalance of normal modes becomes shorter as we change the hopping parameter from $k = 1.0$ and $J = 1.0$ to $k = 1.0$ and $J = 0.5$. Besides, there are fewer coincident peak and dip values of population imbalances.

Our model differs from other autonomous engine designs [17–20, 26] by using the Rabi-like interaction in a fully coupled scheme without RWA. Ground state excitations result in virtual photon generation. In our model, interactions between qubit, cavity, and mechanical mode are employed to generate and amplify the transduction of virtual photons. Amplification by radiation fields leads to the guidance of synchronicity of the virtual photon generation and work extraction. The synchronicity between population imbalances of occupation numbers can be used to harmonize external loads with rotary motion [18–20]. This makes our model plausible in both theoretical and experimental analysis of work in autonomous engine schemes.

4. Conclusion

We investigate autonomous optomechanical systems for fully coupled schemes in the QED framework. Employing the effective model beyond the RWA, we analyze both Rabi-like and piston–mechanical mode interactions in tuning the virtual radiation pressure. Casimir effect and Rabi splitting are analyzed by the avoided crossing in the eigenenergy spectrum. Second order coherence functions are used to see the effect of virtual photon conversion in the cavity and mechanical mode. Work extraction is studied by describing power in terms of the expectation values of the mechanical mode. Then transduction of the radiation field into the mechanical mode is tuned by nonlinear interactions between the piston and mechanical mode in the absence of an external driving field.

Acknowledgment

The author thanks Hakan Erkol and O Teoman Turgut for discussion.

References

- [1] Carnot, S. *Réflexions sur la puissance motrice du feu et sur les machines propres à développer cette puissance*; Bachelier Libraire: Paris, France, 1824 (in French).
- [2] Kondepudi, D.; Prigogine, I. *Modern Thermodynamics, Second Edition*; John Wiley and Sons: Chichester, UK, 2015.
- [3] Jarzynski, C. *Phys. Rev. Lett.* **1997**, *78*, 2690-2693.
- [4] Crooks, G. E. *Phys. Rev. E* **1999**, *60*, 2721-2726.
- [5] Seifert, U. *Rep. Prog. Phys.* **2012**, *75*, 126001.
- [6] Hänggi, P.; Marchesoni, F. *Rev. Mod. Phys.* **2009**, *81*, 387-442.
- [7] Scully, M. O. *Phys. Rev. Lett.* **2002**, *88*, 050602.
- [8] Linden, N.; Popescu, S.; Skrzypczyk, P. *Phys. Rev. Lett.* **2010**, *105*, 130401.
- [9] Horodecki, M.; Oppenheim, J. *Nat. Commun.* **2013**, *4*, 2059.
- [10] Correa, L. A.; Palao, J. P.; Alonso, D.; Adesso, G. *Sci. Rep.* **2014**, *4*, 3949.

- [11] Zhang, K.; Bariani, F.; Meystre, P. *Phys. Rev. Lett.* **2014**, *112*, 150602.
- [12] Gröblacher, S.; Hammerer, K.; Vanner, M. R.; Aspelmeyer, M. *Nature (London)* **2009**, *460*, 724-727.
- [13] Tonner, F.; Mahler, G. *Phys. Rev. E* **2005**, *72*, 066118.
- [14] Youssef, M.; Mahler, G.; Obada, A. S. *Physica E* **2010**, *42*, 454-460.
- [15] Brunner, N.; Linden, N.; Popescu, S.; Skrzypczyk, P. *Phys. Rev. E* **2012**, *85*, 051117.
- [16] Levy, A.; Diósi, L.; Kosloff, R. *Phys. Rev. A* **2016**, *93*, 052119.
- [17] Mari, A.; Farace, A.; Giovannetti, V. *Journal of Physics B* **2015**, *48*, 175501.
- [18] Roulet, A.; Nimmrichter, S.; Taylor, J. M. *Quantum Sci. Technol.* **2018**, *3*, 035008.
- [19] Roulet, A.; Nimmrichter, S.; Arrazola, J. M.; Seah, S.; Scarani, V. *Phys. Rev. E* **2017**, *95*, 062131.
- [20] Seah, S.; Nimmrichter, S.; Scarani, V. *New J. Phys.* **2018**, *20*, 043045.
- [21] Boukobza, E.; Tannor, D. J. *Phys. Rev. E* **2006**, *74*, 063823.
- [22] Weimer, H.; Henrich, M. J.; Rempp, F.; Schröder, H.; Mahler, G. *EPL* **2008**, *83*, 30008.
- [23] Waldherr, G.; Mahler, G. *Phys. Rev. E* **2010**, *81*, 061122.
- [24] Xu, Y. Y. *Phys. Rev. E* **2016**, *94*, 062145.
- [25] Kolář, M.; Ryabov, A.; Filip, R. *Phys. Rev. A* **2016**, *93*, 063822.
- [26] Lörch, N.; Bruder, C.; Brunner, N.; Hofer, P. P. *Quantum Sci. Technol.* **2018**, *3*, 035014.
- [27] Liao, J.; Law, C. K.; Kuang, L.; Nori, F. *Phys. Rev. A* **2015**, *92*, 013822.
- [28] Macri, V.; Ridolfo, A.; Di Stefano, O.; Kockum, A. F.; Nori, F.; Savasta, S. *Phys. Rev. X* **2018**, *8*, 011031.
- [29] Wang, H.; Gu, X.; Liu, Y.; Miranowicz, A.; Nori, F. *Phys. Rev. A* **2015**, *92*, 033806.
- [30] Cirio, M.; Debnath, K.; Lambert, N.; Nori, F. *Phys. Rev. Lett.* **2017**, *119*, 053601.
- [31] Restrepo, J.; Favero, I.; Ciuti, C. *Phys. Rev. A* **2017**, *95*, 023832.
- [32] Stassi, R.; Ridolfo, A.; Di Stefano, O.; Hartmann, M. J.; Savasta, S. *Phys. Rev. Lett.* **2013**, *110*, 243601.
- [33] Garziano, L.; Stassi, R.; Macrí, V.; Kockum, A. F.; Savasta, S.; Nori, F. *Phys. Rev. A* **2015**, *92*, 063830.
- [34] Stassi, R.; Savasta, S.; Garziano, L.; Spagnolo, B.; Nori, F. *New J. Phys.* **2016**, *18*, 123005.
- [35] Blais, A.; Huang, R.; Wallraff, A.; Girvin, S. M.; Schoelkopf, R. J. *Phys. Rev. A* **2004**, *69*, 062320.
- [36] Schuster, D. I.; Houck, A. A.; Schreier, J. A.; Wallraff, A.; Gambetta, J. M.; Blais, A.; Frunzio, L.; Majer, J.; Johnson, B.; Devoret, M. H. et al. *Nature (London)* **2007**, *445*, 515-518.
- [37] Larson, J. *Phys. Rev. A* **2008**, *78*, 033833.
- [38] Didier, N.; Pugnetti, S.; Blanter, Y. M.; Fazio, R. *Phys. Rev. B* **2011**, *84*, 054503.
- [39] O'Brien, M. *J. Phys. C* **1972**, *5*, 2045-2063.
- [40] O'Brien, M. *J. Phys. C* **1983**, *16*, 85-106.
- [41] Dereli, T.; Gül, Y.; Forn-Díaz, P.; Müstecaplıoğlu, Ö. E. *Phys. Rev. A* **2012**, *85*, 053841.
- [42] Gül, Y. *Int. J. Mod. Phys. B* **2016**, *30*, 1650125.
- [43] Gül, Y. *Int. J. Mod. Phys. B* **2018**, *32*, 1850088.
- [44] Levy, A.; Kosloff, R. *Europhys. Lett.* **2014**, *107*, 20004.
- [45] Gardas, B.; Deffner, S. *Phys. Rev. E* **2015**, *92*, 042126.
- [46] Hofer, P. P.; Perarnau-Llobet, M.; Miranda, L. D. M.; Haack, G.; Silva, R.; Brask, J. B.; Brunner, N. *New J. Phys.* **2017**, *19*, 123037.
- [47] Scala, M.; Militello, B.; Messina, A.; Maniscalco, S.; Piilo, J.; Suominen, K. *J. Phys. A* **2007**, *40*, 14527-14536.